Paternally Expressed Gene 10 (PEG10) Promotes Growth, Invasion and Survival of Bladder Cancer

Yoshihisa Kawai[1,2], Kenjiro Imada[1], Shusuke Akamatsu[3], Fan Zhang[1], Roland Seiler[1,4], Tetsutaro Hayashi[1], Jeffrey Leong[1], Eliana Beraldi[1], Neetu Saxena[1], Alexander Kretschmer[1], Htoo Zarni Oo[1], Alberto Contreras[1], Hideyasu Matsuyama[2], Dong Lin[1], Ladan Fazli[1], Colin C. Collins[1], Alexander W. Wyatt[1], Peter C. Black[1], and Martin E. Gleave[1]

[1]The Vancouver Prostate Centre and Department of Urologic Sciences, University of British Columbia, Vancouver, BC, Canada
[2]Department of Urology, Graduate School of Medicine, Yamaguchi University, Ube, Japan
[3]Department of Urology, Kyoto University Graduate School of Medicine, Kyoto, Japan
[4]Department of Urology, University Hospital Bern, Bern, Switzerland

Running title: PEG10 promotes progression of bladder cancer

Keywords: PEG10, bladder cancer, neuroendocrine, chemotherapy resistant, proliferation and invasion

The authors declare no potential conflicts of interest.

This study was supported by a TFRI New Frontiers Program Project Grant (TFRI Project #1062).

Corresponding author: Martin E. Gleave, The Vancouver Prostate Centre and Department of Urologic Sciences, University of British Columbia, 2660 Oak Street, Vancouver, British Columbia V6H 3Z6, Canada. Phone: +1-604-875-4818; Fax: +1-604-875-5654; E-mail: m.gleave@ubc.ca

Abstract

Paternally Expressed Gene 10 (*PEG10*) has been associated with neuroendocrine (NE)-muscle-invasive bladder cancer (MIBC), a subtype of the disease with the poorest survival. In this work, we further characterized the expression pattern of *PEG10* in TCGA database of 412 MIBC pateints, and found that, compared to other subtypes, *PEG10* mRNA level was enhanced in NE-like MIBC and highly correlats with other NE markers. PEG10 protein level also associated with NE markers in a tissue microarray (TMA) of 82 cases. In bladder cancer cell lines, PEG10 expression was induced in drug-resistant compared to parental cells, and knocking-down of PEG10 re-sensitized cells to chemotherapy. Loss of PEG10 increased protein levels of cell cycle regulators p21 and p27 and delayed G1/S transition, while over-expression of PEG10 enhanced cancer cell proliferation. PEG10 silencing also lowered levels of SLUG and SNAIL, leading to reduced invasion and migration. In an orthotopic bladder cancer model, systemic treatment with PEG10 antisense oligonucleotide delayed progression of T24 xenografts. In summary, elevated expression of *PEG10* in MIBC may contribute to the disease progression by promoting survival, proliferation and metastasis. Targeting PEG10 is a novel potential therapeutic approach for a subset of bladder cancers.

Introduction

Muscle-invasive bladder cancer (MIBC) is highly aggressive with poor survival rates (1, 2). Thorough understanding of disease progression is needed to guide treatments for this common, highly lethal malignancy. Recent molecular characterization from the Cancer Genome Atlas (TCGA) identified driver genes and pathways of MIBC (3). Among the many genomic, genetic, and epigenetic modifications, factors targeting *RB1* and *TP53* tumor suppressor genes are the most prevalent (4). 40–50% of MIBC have inactivating mutations or reduced expression of *RB1*, which is strongly associated with poor clinical outcomes (5, 6). Loss-of-function mutations of *TP53* are present in up to 60% of MIBC (7) and are also associated with disease poor outcomes (8, 9). In addition, abnormalities of *RB1* and *TP53* genes coexist among 40–50% of MIBC (10).

Recently, the neuroendocrine (NE)-like subtype of MIBC has been recognized as a subgroup with the poorest survival in MIBC patients (3, 11, 12). These tumors express relatively high levels of NE markers, as well as neuronal differentiation and development genes (3, 11). Interestingly, in the TCGA, unbiased nonnegative matrix factorization (NMF) consensus clustering of RNA-Seq data from 408 tumors revealed Paternally Expressed Gene 10 (PEG10) as one of the genes associated with poor prognosis of NE-like bladder cancers (3). This is in line with previous studies from a patient-derived xenograft model that undergoes transdifferentiation from conventional prostatic adenocarcinoma to NE prostate cancer (NEPC), where PEG10 was identified as a NEPC-specific therapeutic candidate (13). PEG10 promotes growth and invasion of prostate cancer cells, and its expression and function are tightly regulated by *RB1* and *TP53* whose genetic aberrations are hallmarks of NEPC.

PEG10 is a retrotransposon-derived placental gene which structurally resembles human

immunodeficiency virus (14). Although PEG10 no longer retains the reverse transcriptase activity, it is distinct among other mammalian genes by carrying an active −1 ribosomal frameshift element, allowing translation of two isoforms (RF1 and RF1/2) from overlapping reading frames from the same transcript (15). PEG10 also possesses two translation initiation sites, 'a' and 'b', where 'b' is a non-ATG codon; besides this, PEG10 carries a domain for protease activity to generate a distinct self-cleavage product (termed cleaved n-terminal fragment; CNF). All these suggest a highly complex biology for PEG10 (16). Expression of PEG10 is low in adult tissues, but it is essential for placental development; heterozygous knockout *PEG10*+/− mice demonstrate lethality by embryonic day 10.5 (17). In addition to PEG10 proteins, a long noncoding RNA (lncRNA) PEG10 has also been linked to several types of tumors (18, 19).

Since mutations of *TP53* and inactivation of *RB1* are common in MIBC, and because NE gene expression appears to drive a particularly poor prognosis in a subset of patients, we hypothesized that PEG10 may contribute to disease progression and adverse prognosis. To test this hypothesis, we characterized PEG10 function in MIBC progression and investigated PEG10 as a novel therapeutic target in MIBC.

Materials and Methods

Cell lines

Bladder carcinoma cell lines were received from the Pathology Core of the Bladder Cancer SPORE at MD Anderson Cancer Center. Cells were authenticated by DNA fingerprinting using AmpFISTR Amplification or AmpFISTR Profiler PCR Amplification protocols (Life Technologies). Cells were maintained in MEM supplemented with 10% FBS, penicillin, streptomycin, vitamins, L-glutamine, nonessential amino acids and pyruvate supplements, and routinely tested for mycoplsma.

Analysis of The Cancer Genome Atlas dataset

DNA sequencing results for *RB1* and *TP53*, including calls for deep deletions, truncation and missense mutations, as well as normalized RNAseq-derived gene expression data for *PEG10* and NE markers were downloaded from cbioportal.org (3). *PEG10* expression as analyzed between different molecular subtypes (mRNA clusters (3)) and correlation with other NE markers was calculated dependent on molecular subtype as well as *RB1* and *TP53* gene status.

Tissue Microarray (TMA) and Immunohistochemistry (IHC)

The Vancouver Prostate Centre (VPC) Bladder Cancer TMA consists of 21 cases of MIBC and 61 cases of NMIBC specimens obtained by transurethral resection. Written consents have been obtained from the patients and the study was performed following the ethical guidelines of University of British Columbia (UBC) CREB (# H09-01628) and reviewed by the Chair of the UBC Clinical Research Ethics Board. TMA preparation and IHC was performed as described previously(20, 21) and as outlined in the Supplementary Information. PEG10 IHC staining in the TMA was scored as: 0 = no staining, 1 = faint or focal staining, 2 = convincing intensity in a minority of cells, and 3 = convincing intensity in a majority of cells.

Western blotting and quantitative real-time qPCR

Western blotting and real-time qPCR were conducted as described before (22, 23) and as outlined in the Supplementary Data. Primary antibodies and probes used in this study were shown in the Supplementary Table S1 and S2, respectively.

Transfections

Transfections of siRNAs (listed in the Supplementary Table S3) were carried out using RNAiMAX (Life Technologies) following the manufacturer's instruction. A PEG10-antisense oligonucleotide (ASO, 5′-GGCAGTGGTAGCGGCAGTAT-3′) and scrambled oligonucleotide (SCRB, 5′-CCTTCCCTGAAGGTTCCTCC-3′) were purchased from IONIS Pharmaceuticals and transfected using Oligofectamin following protocols described previously (24). PEG10 plasmids were generated as described previously (13). All plasmids were transfected using Lipofectamin (Life Technologies) following the manufacturer's instruction.

Proliferation and cell cycle analysis

Cell growth was evaluated with a Cell Counting Kit 8 (Dojindo) following the manufacturer's instruction. The cell cycle distribution was examined by double stainings with bromodeoxyuridine (BrdU) and 7-Aminoactinomycin D (7-AAD) using a BrdU-FITC Flow Kit (BD Biosciences) following the manufacturer's instruction. The double thymidine block was performed as described previously (13).

Cell migration and invasion assays

For migration assays, scratches were made using a sterilized aerosol pipet tip, and cells were maintained in serum-free medium which contains TGF-β (0.1 ng/ml) for 24 h. Mitomycin C (0.3 μg/ml) was added after scratching to suppress cell growth. Bright field images were taken at the same area right after the scratch and also at 24h after the scratch. Cell invasion was

investigated using Biocoat Matrigel invasion chambers (BD Biosciences). Briefly, 5×10^4 cells were plated in the upper chamber with serum-free condition, and medium containing 20% FBS was set in the lower chamber. At 18 hours after seeding, the polycarbohydrate membranes from the bottom of the upper chambers were dissected, fixed with methanol, and then stained with crystal violate to visualize the invaded cells. The number of invading cells was quantified in four microscopic fields and averaged.

Orthotopic bladder cancer xenograft model

The animal work was approved by the Review Board of UBC (Vancouver, Canada) (A14-0291). Procedures were performed as described previously (25). Six-week-old female nude mice (Harlan Laboratories, Indianapolis, IN) were anesthetized using 2% isoflurane. Analgesia was achieved by a subcutaneous injection of meloxicam (Boehringer Ingelheim Vetmedica, St. Joseph, MO). 4.0×10^5 cells in 50 µL Matrigel suspension were inoculated into the bladder wall of nude mice using a 30 G needle by percutaneous injection under ultrasound guidance. Beginning on 4^{th} day after tumor inoculation, 15 mg/kg of PEG10- or Scr-ASO were administerd systemically via intraperitoneal injection once per day for 5 days and then 3 times per week thereafter. For *in vivo* photoimaging (IVIS Lumina, PerkinElmer), cells transfected with a lentiviral construct for a firefly luciferase gene under Blasticidin selection (Life Technologies) were employed. The direct association between the cell number, luciferase activity, tumor size, and bioluminescence was screened and controlled ($R>0.99$) as described before (25) using the Xenogen IVIS Spectrum imager. Bioluminescence using the Xenogen IVIS Spectrum imaging system (Perkin Elmer, Waltham, MA) was used to assess tumor burden. Images were recorded at 10 and 15 minutes after luciferin injection. Averaged counts were used for statistical analysis. The TUNEL assay was outlined in the Supplementar Data.

Statistics

Statistical analyses were carried out using the chi-square test, the unpaired t-test, the analysis of variance, and Wilcoxon test using JMP9 software (SAS Institute, Cary, NC). Statistical significance was determined as $p < 0.05$.

Results

PEG10 associates with NE markers in bladder cancer

The expression pattern of *PEG10* was investigated in MIBC cases from the TCGA database, which consists of 408 samples with RNA-Seq data from chemotherapy-naïve, muscle-invasive, high-grade urothelial tumors (3). *PEG10* mRNA was highly expressed in the neuronal subtype (NE-like) MIBC compared to the Basal, Luminal, Luminal-infiltrated and Luminal-papillary subtypes (Fig. 1A). Furthermore, *PEG10* mRNA levels correlated with NE markers in an all cases analysis (Fig. 1B). This correlation was seen especially in cases with loss of *RB1/TP53* (Supplementary Fig. S1A), but became less significant in cases with wild type (WT) *RB1/TP53* (Supplementary Fig. S1A). The observation that PEG10 associated with NE markers in bladder cancer is consistent with other reports from both prostate (13, 26) (Supplementary Fig. S1B) and small cell lung cancer (27, 28), suggesting a broad positive correlation between PEG10 and NE phenotypes. This finding was further confirmed in the bladder cancer TMA from the VPC, which demonstrated positive correlation between PEG10 protein and NE markers (Fig. 1C).

Since *TP53* and *RB1* inactivation are common in MIBC (3, 29, 30), and *PEG10* is a known target gene of RB/E2F and p53 (13, 31, 32), we next explored if *PEG10* mRNA levels correlate with the status of *RB1/TP53* in the TCGA database. As shown in Fig. 1D, *PEG10* expression is enhanced in cases with *RB1/TP53* loss (left panel), and this increase was further magnified in the 20 NE-like cases (right panel). Interestingly, although *PEG10* mRNA was not significantly correlated with overall survival (OS) in an analysis of all cases or when substratified by *RB1/TP53* loss (Supplementary Fig. S1C), there was a statistically insignificant suggestion of worse survival with increased PEG10 mRNA levels in the 20 NE-like cases (Fig.

1E).

PEG10 levels are elevated in chemotherapy-resistant cells

To define roles for PEG10 in bladder cancer progression, we first examined mRNA and protein levels of PEG10 in a panel of bladder cancer cell lines (33) by real-time quantitative PCR (qPCR) (Fig. 2A) and western blotting (Fig. 2B). UM-UC14 and T24 cells showed high levels of PEG10 RF1/2 and RF1 isoforms (Fig. 2B). The levels of CNF1/2 isoforms were low in all bladder cancer cell lines (Fig. 2B). Since loss of *RB1* and *TP53* plays an important role during NE transdifferentiation in prostate cancer (13), we therefore compared RB and *TP53* status with PEG10 levels in these bladder cancer cell lines. Five out of seven cell lines carry *TP53* mutations (mt) and two of the cell lines displayed undetectable phospho-Rb protein (pRb, Fig. 2B). Interestingly, UM-UC14 cells, which were featured with both mt *TP53* and loss of Rb, showed highest mRNA and protein levels of PEG10 (Fig. 2A and 2B). Next we explored whether manipulation of *TP53* status would modulate the PEG10 level in bladder cancer cells. Introduction of wild type (WT) *TP53* into T24 cells (with mt *TP53* and pRb protein) significantly attenuated both mRNA and protein levels of PEG10 (Fig. 2C and 2D). In contrast, introduction of WT *TP53* in UM-UC14 cells (with mt *TP53* and no pRb protein) did not significantly affect the PEG10 level (Supplementary Fig. S2A).

Since elevated PEG10 levels associate with NE-like tumors, which display the poorest prognosis in MIBC, we hypothesized that PEG10 may regulate sensitivity of bladder cancer cells to chemotherapy. We therefore investigated if PEG10 contributes to acquired chemotherapy resistance by establishing a stable cisplatin (CDDP)-resistant T24 cell line (T24R) that maintains constant growth rate in the presence of 10 μM of CDDP for at least 3 months (34). Both PEG10 protein and mRNA levels were highly elevated in resistant, compared to parental, cells (Fig. 2E).

In addition, PEG10 was significantly induced by CDDP over 5 days (Fig. 2F, G), indicating that induction of PEG10 might be an early event contributing to development of resistance. A similar phenomenon was observed in UM-UC14 cells (Supplementary Fig. S2B). PEG10 silencing triggered cell death in T24R cells to a greater extent than that in the parental cells, as measured by PARP cleavage (c-PARP, Fig. 2H); loss of PEG10 also retarded growth of the resistant T24R cells (Supplementary Fig. S2C), suggesting that PEG10 may promote bladder cancer cell growth and survival after chemotherapy.

Besides CDDP, taxanes are also frequently used as second-line therapy of advanced MIBC. We developed a stable paclitaxel-resistant T24 cell line (Paclitaxel-Re) by culturing cells with increasing concentrations of paclitaxel (starting from 0.125 μM) with 2-fold increase of each cycle and eventually maintained cells at 2 μM paclitaxel. The resistant cell line also exhibited increased PEG10 mRNA and protein levels compared to parental cells (Supplementary Fig. S2D), and PEG10 silencing triggered cell death in the resistant cells to a gretaer extent than in the parental cell line (Supplementary Fig. S2E), again indicating that chemotherapy-resistant cancer cell lines become more dependent on PEG10 for survival. Interestingly, analysis from a neoadjuvant chemotherapy (NAC) cohort (12, 35) revealed that, while mRNA levels of *PEG10* were not predictive of response to NAC in the all case-analysis (Supplementary Fig. S2F, left panel), there was an enrichment of *PEG10* in the post-NAC luminal-like tumors, which had higher *PEG10* levels compared to matched pre-NAC tumors (Supplementary Fig. S2F, middle and right panels).

PEG10 triggers Rb phosphorylation and promotes proliferation of bladder cancer cells

To further define roles for PEG10 in bladder cancer progression, we examined effects of PEG10 on cell proliferation in T24 cells which carry mt *TP53* and pRb protein. PEG10 silencing

attenuated T24 cell growth (Fig. 3A) enhancing levels of the cell cycle regulators p21 and p27 and reducing cyclin D1 and pRb protein (Fig. 3B). Effects of PEG10 on cell cycle progression were further evaluated in T24 cells using a BrdU incorporation assay in combination with 7-AAD staining in the cells released from thymidine block. As shown in the cell cycle population bar graph (Fig. 3C) and the FACS profile (Supplementary Fig. S3A), siPEG10 delayed re-entry of cells from G1 to S phase. Analysis with Western blot indicated that Rb was hypo-phosphorylated after PEG10 silencing (Fig. 3D), likely due to increased p21 and p27 protein levels (Fig. 3D). Congruent with these observations, over-expression of PEG10 isoforms RF1 or RF1/2 in T24 cells promoted Rb phosphorylation and triggered cell growth (Fig. 3E, F).

PEG10 promotes proliferation of bladder cancer cells when tRb protein is absent

The above findings indicate that PEG10 facilitates Rb phosphorylation to promote cell cycle progression. We next investigated if PEG10 modulates proliferation in bladder cancer cells lacking tRb protein (Fig. 2B). UM-UC14 cells bear mt *TP53* and have no Rb protein, so that E2F transactivation is left unsupervised by Rb pathway. PEG10 silencing in UM-UC14 cells still repressed cell growth and induced p21 and p27 proteins (Fig. 4A, 4B). In the BrdU and 7-AAD combination assay, inhibition of PEG10 delayed entry of cells into S phase after being released from the thymidine blocking (Fig. 4C, Supplementary Fig. S4A), elevating levels of p21 and p27 (Fig. 4D). In contrast, overexpression of PEG10 promoted UM-UC14 cell growth (Fig. 4E, F). In another cell line UM-UC6, which carries WT *TP53* and expresses tRb but not pRb protein so that E2F might be repressed by the Rb pathway, PEG10 overexpression still enhanced cell growth (Supplementary Fig. S4B, S4C). These data indicate that PEG10 promotes proliferation through molecular mechanisms involving Rb-dependent and Rb-independent pathways.

PEG10 promotes migration and invasion of bladder cancer cells

Considering the critical role of PEG10 in placental development where invasion of the maternal tissue presents a fundamental step (17), we next investigated roles of PEG10 on migration and invasion of bladder cancer cells. Firstly, T24 and UM-UC14 cells transfected with siPEG10s or siCtrl were assessed in a migration assay using the wound healing method. As shown in Fig. 5A, PEG10 silencing restrained cell migration, while, in contrast, overexpression of PEG10 accelerated cell migration (Supplementary Fig. S5A). Next, T24 and UM-UC14 cells transfected with PEG10 siRNAs or siCtrl were applied to an invasion assay recruiting the Biocoat Matrigel invasion chambers. Cells were stained with crystal violet (Fig. 5B) and numbers of invaded cells were quantified under microscopy (Fig. 5C). Enumeration results indicate that PEG10 silencing significantly reduced invasion of bladder cancer cells.

To define molecular mechanisms of PEG10 modulation of migration and invasion in bladder cancer cells, protein levels of key regulators of cell mobility were investigated. Interestingly, TGF-β treatment, which is known to stimulate the epithelial-to-mesenchymal transition (EMT), induced PEG10 protein and also the levels of SLUG and SNAIL (Fig. 5D), two key regulators of EMT (36). PEG10 silencing reduced TGF-β-stimulated SLUG and SNAIL protein levels (Fig. 5D), whereas PEG10 overexpression enhanced levels of these proteins (Supplementary Fig. S5B), indicating that PEG10 mediates TGF-β-induced EMT via SLUG and SNAIL-dependent pathways.

***PEG10* knockdown attenuates *in vivo* tumor growth**

The above studies suggest that PEG10 may trigger bladder cancer progression by promoting survival (Fig. 2), proliferation (Fig. 3 and 4) and invasion (Fig. 5). We next evaluated whether targeting PEG10 with antisense oligonucleotides (ASO) can retard tumor progression. Firstly, we assessed effects of PEG10-ASO in T24 cells *in vitro*. PEG10-ASO reduced both

mRNA and protein levels of PEG10 (Fig. 6A, Supplementary Fig. S6A) in a dose- and sequence-dependnet manner, and suppressed growth of T24 cells (Fig. 6B).

Next, an orthotopic bladder cancer xenograft model using T24 cells was established to evaluate effects of PEG10 inhibition *in vivo*. Tumor-bearing mice were treated with PEG10-ASO or Scrambled-ASO (Scr-ASO), and tumor burden was monitored with bioluminescence using the *In Vivo* Imaging Spectrum (IVIS) and with tumor volume using ultrasonography. PEG10-ASO significantly delayed tumor growth compared to scrambled controls (Fig. 6C, D, E). Furthermore, enhanced TUNEL staining signal was observed in the PEG10-ASO-treated tumor samples, suggesting increased apoptotic rates post PEG10-ASO treatment (Fig. 6F). IHC staining and western blot on excised tumor tissues confirmed the reduction of PEG10 levels in the ASO-treated tumors (Supplementary Fig. S6B, S6C).

Discussion

This study demonstrates that PEG10 is associated with invasive bladder cancer and that targeting PEG10 represses tumor progression in both *in vitro* and *in vivo* models. *PEG10* is a placental gene essential for the development of mammalian placentation (17). Therefore, the origin of PEG10 is of interest considering its role on promoting migration and invasion of cancer cells (Fig. 5). PEG10 may also be oncogenic by modulating cell cycle progression (37), reducing apoptosis mediated by SIAH1 (38), and/or by impeding TGF-β signaling via interaction with TGF-β receptor ALK1 (39). PEG10 presents a wide diversity of functions regulating cell growth and differentiation in addition to its key role in placental formation.As a potent growth promoter, PEG10 expression is tightly controlled. *PEG10* gene is imprinted in the placenta/embryo and its expression is silenced in adult tissues. However, the expression of PEG10 is significantly

enhanced in the NE-like subtype of bladder cancer (Fig. 1A, B, C), a subtype which displays the poorest survival among the patients. Neuroendocrine differentiation is characterized by deregulated *TP53* and *RB1*, and PEG10 is known to be re-expressed to drive proliferation and migration of cancer cells when left unchecked in the context of deregulated *TP53* and *RB1* pathways. While PEG10 does not directly contribute to NE transdifferentiation (13), alterations in WT *TP53* and tRb in NE-like tumors de-repress PEG10 expression to enhance proliferation, survival and migration of NE-like tumors. In addition to altered transcriptional regulation, PEG10 may also undergo translational and post-translational regulation that controls the protein level of PEG10 in cancer cells.

This study also links PEG10 to acquired chemotherapy resistance. PEG10 is induced in the bladder cancer cells after transient CDDP and paclitaxel treatments and remains at high levels in stable drug-resistant cell lines. Silencing of PEG10 by siRNAs re-sensitizes treatment-resistant cancer cells to chemotherapy, indicating a role for PEG10 in stress responses and survival. Cancer cells stressed by treatment need to reprogram the transcriptome to adapt to varied microenvironments; reactivation of PEG10 is representative of lineage plasticity through activation of developmental pathways activation that support acquired treatment-resistance in cancer. The unique genomic features (*TP53, RB1*) of PEG10 regulation, along with its absence in most adult tissues, oncogenic characteristics, and intimate association with aberrant cancer cells, make it a distinct therapeutic target for a subset of advanced bladder cancers. While these data provide preclinical proof of principle for PEG10 inhibition in subtypes of advanced bladder cancer, assessment of PEG10 ASO combined with chemotherapy in preclinical models is required to further define clinical development path and roles of PEG10 in treatment response and resistance.

The ability of PEG10 to promote proliferation in both Rb functioning- and Rb absent-bladder cancer cells is of interest. Cellular division is well known to be controlled at the G1 to S phase transition by the Rb protein. Rb interacts with E2F and represses its transactivation of cell cycle-regulating genes necessary for cellular division (40). During G1-S transition, Rb protein is phosphorylated by cyclin-dependent kinases and their partners to release E2F protein from its suppression, allowing S phase entry. The G1 arrest, however, does not always rely on Rb family members. Mouse embryos with triple knockout (TKO) of Rb protein and two family members p107 and p130 live until days 9–11 of gestation, and the ability of TKO cells to arrest in G0/G1 is associated with repression of key E2F target genes (41), suggesting Rb-independent mechanisms regulating E2F transactivation. Mutations or deletion of *RB1* are common in cancer, allowing escape from the antioncogenic senescence program. How Rb-negative tumor cells control proliferation rates in stressed environments remains undefined. The broad role of PEG10 in regulating proliferation in both Rb-functional and Rb-absent bladder cancer cells provide another rational for molecular targeted therapy. Further study is required to define molecular mechanisms by which PEG10 regulates G1-S transition in Rb-negative cells.

In conclusion, we demonstrate that PEG10 is associated with poor prognostic NE subtype of bladder cancer, promoting cell survival, proliferation and invasion. Inhibition of PEG10 may be a novel treatment strategy for certain subset of bladder cancers.

Disclosure of Potential Conflicts of Interest

No conflicts of interest were disclosed.

Authors' Contributions

Conception and design: S. Akamatsu, M.E. Gleave, P.C. Black, A.W. Wyatt, C.C. Collins, Y. Kawai, F. Zhang

Development of methodology: S. Akamatsu, Y. Kawai, F. Zhang, R. Seiler

Acquisition of data (provided animals, acquired and managed patients, provided facilities, etc.): Y. Kawai, K. Imada, S. Akamatsu, F. Zhang, R. Seiler, J. Leong, E. Beraldi, N. Saxena, A. Kretschmer, L. Fazli

Analysis and interpretation of data (e.g., statistical analysis, biostatistics, computational analysis): S. Akamatsu, Y. Kawai, R. Seiler, F. Zhang

Writing, review, and/or revision of the manuscript: Y. Kawai, S. Akamatsu, M.E. Gleave, P.C. Black, A.W. Wyatt, F. Zhang, R. Seiler

Administrative, technical, or material support (i.e., reporting or organizing data, constructing databases): T. Hayashi, H.Z. Oo, A. Contreras, H. Matsuyama, D. Lin

Supervision: M.E. Gleave

Acknowledgments

We thank Estelle Li, Igor Moskalev, Charan Tse, Joanna Pan, Brian Lee, and Teresa Huang for technical assistance. This study was supported by a Terry Fox Research Institute New Frontiers Program Project Grant (TFRI Project #1062) for the whole author team.

References

1. Alfred Witjes J, Lebret T, Comperat EM, Cowan NC, De Santis M, Bruins HM, et al. Updated 2016 EAU Guidelines on Muscle-invasive and Metastatic Bladder Cancer. European urology. 2017;71(3):462-75.
2. Black P, So A. Perioperative chemotherapy for muscle-invasive bladder cancer. Can Urol Assoc J. 2009;3(6 Suppl 4):S223-7.
3. Robertson AG, Kim J, Al-Ahmadie H, Bellmunt J, Guo G, Cherniack AD, et al. Comprehensive Molecular Characterization of Muscle-Invasive Bladder Cancer. Cell. 2017;171(3):540-56 e25.
4. Cordon-Cardo C. p53 and RB: simple interesting correlates or tumor markers of critical predictive nature? J Clin Oncol. 2004;22(6):975-7.
5. Logothetis CJ, Xu HJ, Ro JY, Hu SX, Sahin A, Ordonez N, et al. Altered expression of retinoblastoma protein and known prognostic variables in locally advanced bladder cancer. J Natl Cancer Inst. 1992;84(16):1256-61.
6. Cordon-Cardo C, Wartinger D, Petrylak D, Dalbagni G, Fair WR, Fuks Z, et al. Altered expression of the retinoblastoma gene product: prognostic indicator in bladder cancer. J Natl Cancer Inst. 1992;84(16):1251-6.
7. Cordon-Cardo C, Reuter VE. Alterations of tumor suppressor genes in bladder cancer. Semin Diagn Pathol. 1997;14(2):123-32.
8. Esrig D, Elmajian D, Groshen S, Freeman JA, Stein JP, Chen SC, et al. Accumulation of nuclear p53 and tumor progression in bladder cancer. N Engl J Med. 1994;331(19):1259-64.
9. Soini Y, Turpeenniemi-Hujanen T, Kamel D, Autio-Harmainen H, Risteli J, Risteli L, et al. p53 immunohistochemistry in transitional cell carcinoma and dysplasia of the urinary bladder correlates with disease progression. Br J Cancer. 1993;68(5):1029-35.
10. He F, Mo L, Zheng XY, Hu C, Lepor H, Lee EY, et al. Deficiency of pRb family proteins and p53 in invasive urothelial tumorigenesis. Cancer Res. 2009;69(24):9413-21.
11. Sjodahl G, Eriksson P, Liedberg F, Hoglund M. Molecular classification of urothelial carcinoma: global mRNA classification versus tumour-cell phenotype classification. The Journal of pathology. 2017;242(1):113-25.
12. Seiler R, Gibb EA, Wang NQ, Oo HZ, Lam HM, van Kessel KE, et al. Divergent Biological Response to Neoadjuvant Chemotherapy in Muscle-invasive Bladder Cancer. Clin Cancer Res. 2018.
13. Akamatsu S, Wyatt AW, Lin D, Lysakowski S, Zhang F, Kim S, et al. The Placental Gene PEG10 Promotes Progression of Neuroendocrine Prostate Cancer. Cell Rep. 2015;12(6):922-36.
14. Ono R, Kobayashi S, Wagatsuma H, Aisaka K, Kohda T, Kaneko-Ishino T, et al. A retrotransposon-derived gene, PEG10, is a novel imprinted gene located on human chromosome 7q21. Genomics. 2001;73(2):232-7.
15. Clark MB, Janicke M, Gottesbuhren U, Kleffmann T, Legge M, Poole ES, et al. Mammalian gene PEG10 expresses two reading frames by high efficiency -1 frameshifting in embryonic-associated tissues. J Biol Chem. 2007;282(52):37359-69.
16. Lux H, Flammann H, Hafner M, Lux A. Genetic and molecular analyses of PEG10 reveal new aspects of genomic organization, transcription and translation. PLoS One. 2010;5(1):e8686.
17. Ono R, Nakamura K, Inoue K, Naruse M, Usami T, Wakisaka-Saito N, et al. Deletion of Peg10, an imprinted gene acquired from a retrotransposon, causes early embryonic lethality. Nat Genet. 2006;38(1):101-6.
18. Zang W, Wang T, Huang J, Li M, Wang Y, Du Y, et al. Long noncoding RNA PEG10 regulates proliferation and invasion of esophageal cancer cells. Cancer Gene Ther. 2015;22(3):138-44.
19. Jiang F, Qi W, Wang Y, Wang W, Fan L. lncRNA PEG10 promotes cell survival, invasion and migration by sponging miR-134 in human bladder cancer. Biomed Pharmacother. 2019;114:108814.
20. Lamoureux F, Baud'huin M, Ory B, Guiho R, Zoubeidi A, Gleave M, et al. Clusterin inhibition using OGX-011 synergistically enhances zoledronic acid activity in osteosarcoma. Oncotarget. 2014;5(17):7805-19.
21. Shiota M, Bishop JL, Nip KM, Zardan A, Takeuchi A, Cordonnier T, et al. Hsp27 regulates epithelial mesenchymal transition, metastasis, and circulating tumor cells in prostate cancer. Cancer research. 2013;73(10):3109-19.
22. Gust KM, McConkey DJ, Awrey S, Hegarty PK, Qing J, Bondaruk J, et al. Fibroblast growth factor receptor 3 is a rational therapeutic target in bladder cancer. Mol Cancer Ther. 2013;12(7):1245-54.
23. Matsumoto H, Yamamoto Y, Shiota M, Kuruma H, Beraldi E, Matsuyama H, et al. Cotargeting Androgen Receptor and Clusterin Delays Castrate-Resistant Prostate Cancer Progression by Inhibiting Adaptive Stress Response and AR Stability. Cancer Res. 2013;73(16):5206-17.

24. Sowery RD, Hadaschik BA, So AI, Zoubeidi A, Fazli L, Hurtado-Coll A, et al. Clusterin knockdown using the antisense oligonucleotide OGX-011 re-sensitizes docetaxel-refractory prostate cancer PC-3 cells to chemotherapy. BJU Int. 2008;102(3):389-97.
25. Jager W, Moskalev I, Janssen C, Hayashi T, Awrey S, Gust KM, et al. Ultrasound-guided intramural inoculation of orthotopic bladder cancer xenografts: a novel high-precision approach. PLoS One. 2013;8(3):e59536.
26. Haram KM, Peltier HJ, Lu B, Bhasin M, Otu HH, Choy B, et al. Gene expression profile of mouse prostate tumors reveals dysregulations in major biological processes and identifies potential murine targets for preclinical development of human prostate cancer therapy. The Prostate. 2008;68(14):1517-30.
27. Kastner S, Voss T, Keuerleber S, Glockel C, Freissmuth M, Sommergruber W. Expression of G protein-coupled receptor 19 in human lung cancer cells is triggered by entry into S-phase and supports G(2)-M cell-cycle progression. Mol Cancer Res. 2012;10(10):1343-58.
28. Takeuchi T, Tomida S, Yatabe Y, Kosaka T, Osada H, Yanagisawa K, et al. Expression profile-defined classification of lung adenocarcinoma shows close relationship with underlying major genetic changes and clinicopathologic behaviors. J Clin Oncol. 2006;24(11):1679-88.
29. Cordon-Cardo C. p53 and RB: simple interesting correlates or tumor markers of critical predictive nature? Journal of clinical oncology : official journal of the American Society of Clinical Oncology. 2004;22(6):975-7.
30. He F, Mo L, Zheng XY, Hu C, Lepor H, Lee EY, et al. Deficiency of pRb family proteins and p53 in invasive urothelial tumorigenesis. Cancer research. 2009;69(24):9413-21.
31. Spurgers KB, Gold DL, Coombes KR, Bohnenstiehl NL, Mullins B, Meyn RE, et al. Identification of cell cycle regulatory genes as principal targets of p53-mediated transcriptional repression. The Journal of biological chemistry. 2006;281(35):25134-42.
32. Wang C, Xiao Y, Hu Z, Chen Y, Liu N, Hu G. PEG10 directly regulated by E2Fs might have a role in the development of hepatocellular carcinoma. FEBS Lett. 2008;582(18):2793-8.
33. Hayashi T, Gust KM, Wyatt AW, Goriki A, Jager W, Awrey S, et al. Not all NOTCH Is Created Equal: The Oncogenic Role of NOTCH2 in Bladder Cancer and Its Implications for Targeted Therapy. Clin Cancer Res. 2016;22(12):2981-92.
34. Hayashi T, Seiler R, Oo HZ, Jager W, Moskalev I, Awrey S, et al. Targeting HER2 with T-DM1, an Antibody Cytotoxic Drug Conjugate, is Effective in HER2 Over Expressing Bladder Cancer. J Urol. 2015;194(4):1120-31.
35. Seiler R, Ashab HAD, Erho N, van Rhijn BWG, Winters B, Douglas J, et al. Impact of Molecular Subtypes in Muscle-invasive Bladder Cancer on Predicting Response and Survival after Neoadjuvant Chemotherapy. European urology. 2017;72(4):544-54.
36. Lamouille S, Xu J, Derynck R. Molecular mechanisms of epithelial-mesenchymal transition. Nat Rev Mol Cell Biol. 2014;15(3):178-96.
37. Tsou AP, Chuang YC, Su JY, Yang CW, Liao YL, Liu WK, et al. Overexpression of a novel imprinted gene, PEG10, in human hepatocellular carcinoma and in regenerating mouse livers. J Biomed Sci. 2003;10(6 Pt 1):625-35.
38. Okabe H, Satoh S, Furukawa Y, Kato T, Hasegawa S, Nakajima Y, et al. Involvement of PEG10 in human hepatocellular carcinogenesis through interaction with SIAH1. Cancer Res. 2003;63(12):3043-8.
39. Lux A, Beil C, Majety M, Barron S, Gallione CJ, Kuhn HM, et al. Human retroviral gag- and gag-pol-like proteins interact with the transforming growth factor-beta receptor activin receptor-like kinase 1. J Biol Chem. 2005;280(9):8482-93.
40. Dick FA, Rubin SM. Molecular mechanisms underlying RB protein function. Nat Rev Mol Cell Biol. 2013;14(5):297-306.
41. Wirt SE, Adler AS, Gebala V, Weimann JM, Schaffer BE, Saddic LA, et al. G1 arrest and differentiation can occur independently of Rb family function. J Cell Biol. 2010;191(4):809-25.

Figure legends

Figure 1. PEG10 associates with NE markers in bladder cancer. **A,** Expression pattern of *PEG10* mRNA in various mRNA expression subtypes of MIBC from the TCGA database. *, $p < 0.01$ compared to the NE-like subtype. **B,** Correlation between *PEG10* mRNA and NE markers in the TCGA dataset. The scale bar (red to blue) indicates the correlation coefficient value. The point plot represents the given correlation coefficient for the given pair, the larger the point, the smaller the p-value. A cross means that the p-value was above 0.05. **C,** PEG10 protein level correlates with NE markers CGA, SYP and ENO2 in the TMA. Representative images were shown in the top panle and the statistical analysis data was shown in bottom. Scale bar: 60 μm. **D,** Association of *PEG10* mRNA with status of *RB1/TP53* in the all case-analysis and the NE-like case-analysis in the TCGA database. **E,** *PEG10* mRNA associates with poorer prognosis in the 20 NE-like patients in the TCGA database.

Figure 2. PEG10 levels are elevated in chemotherapy-resistant cells. **A,** Levels of *PEG10* mRNA as measured with qPCR. Values are normalized to *GAPDH* and expressed as means ± SD, n=3. **B,** Protein levels of PEG10, p53, phospho-Rb (pRb) and total Rb (tRb) were examined with western blotting. Status of *TP53* gene and pRb protein from literature were shown. *, not reported. **C** and **D,** T24 cells were transfected with empty vector (mock) or a plasmid expressing WT *TP53*, and PEG10 protein and mRNA levels were examined with western blotting (**C**) and qPCR (**D**), n=3. *, $p = 0.01$. **E,** PEG10 protein levels and mRNA levels were examined in the stable CDDP-resistant (T24R) and parental T24 cells, n=3. **F,** T24 cells were treated with various doses of CDDP at day 1 and day3. Protein lysates were collected at day 5 and PEG10 protein levels were examined. **G,** T24 cells were treated with CDDP (3 μM) for indicated days and PEG10 protein levels were investigated. H, siRNAs targeting PEG10 or the scrambled siCtrl

were transfected into the T24R and T24 cells. Whole-cell protein lysates were collected 48 hrs after the transfection and the levels of indicated proteins were investigated.

Figure 3. PEG10 triggers phosphorylation of Rb protein and promotes the proliferation of cancer cells. **A,** Cell growth status of T24 cells were monitored with Cell Counting Kit 8 after PEG10 knockdown. Values were normalized to 4 hr after the transfection and shown as mean ± SD, n=3. **B,** Levels of PEG10 and cell cycle regulators were examined in T24 cells transfected with siRNAs. **C,** Cell cycle evaluation by FACS using BrdU incorporation and 7-AAD staining in T24 cells after PEG10 silencing. Cells were initially synchronized at G0/G1 by double thymidine blockade and then released and collected after 3 hrs. The bar graph demonstrates the distribution of the cell population of each phase of the cell cycle, n=3. **D,** Immunoblots showed modulations of G1/S-regulating proteins in cells released from the thymidine block with or without PEG10 silencing. **E,** Effect of PEG10 isoforms overexpression on the growth of T24 cells as investigated as in (**A**). Values are shown as mean ± SD, n=3. **F,** Levels of cell cycle regulators were examined in the PEG10 overexpressing T24 cells.

Figure 4. PEG10 promotes proliferation of bladder cancer cells when pRb protein is absent. **A,** Cell growth status was measured after PEG10 silencing in UM-UC14 cells. Values were shown as mean ± SD, n=3. **B,** Levels of PEG10 and cell cycle regulators were examined after PEG10 knockdown. **C,** Cell cycle analysis by FACS using BrdU incorporation and 7-AAD staining in UM-UC14 cells after PEG10 silencing, n=3. **D,** Immunoblots showed modulations of cell cycle regulating proteins in UM-UC14 cells. **E,** Effect of overexpression of PEG10 on the growth of UM-UC14 cells as monitored with Cell Counting Kit 8. Values are shown as mean ± SD, n=3. **F,** Protein levels of PEG10 and cell cycle regulators were examined in the PEG10 overexpressing UM-UC14 cells.

Figure 5. PEG10 promotes migration and invasion of bladder cancer cells. **A,** T24 and UM-UC-14 cells transfected with siPEG10 or siCtrl were applied to scratch assays with TGF-β stimulation. Representative images of the wounded area were shown. Scale bar: 500 μm. **B,** T24 and UM-UC-14 cells transfected with siPEG10 or siCtrl were applied to the Biocoat Matrigel invasion chambers. Cells invaded to the polycarbohydrate membranes were visulized with crystal violet, and the representative images were shown. **C,** The numbers of invaded cells in four microscopic fields (20x lens) were quantified and shown as mean ± SD, n=3. *, $p < 0.05$ (compared to siCtrl). Scale bar: 500 μm. **D,** Protein levels of invasion- / migration-related regulators were examined from siPEG10 or siCtrl transfected T24 and UM-UC-14 cells.

Fig. 6. *PEG10* knockdown attenuates *in vivo* tumor growth. **A,** PEG10-ASO reduced PEG10 protein level in T24 cells. **B,** PEG10-ASO suppressed growth of T24 cells. The values were shown as mean ± SD, n=3. **C** and **D,** PEG10-ASO attenuated tumor growth of T24 cell xenograft model, as measured with bioluminescence (**C**) and tumor volume (**D**) in the orthotopic bladder tumor model. Values were presented as mean ± SD. **E,** Tumor volumes as monitored using IVIS. Values were expressed as mean ± SD. **F,** Quantification of TUNEL IHC staining in the tumors. Values were expressed as means ± SD.

Fig. 1

A

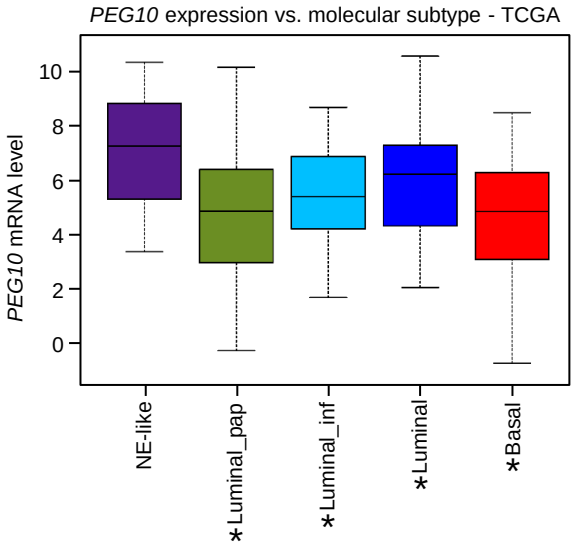

B

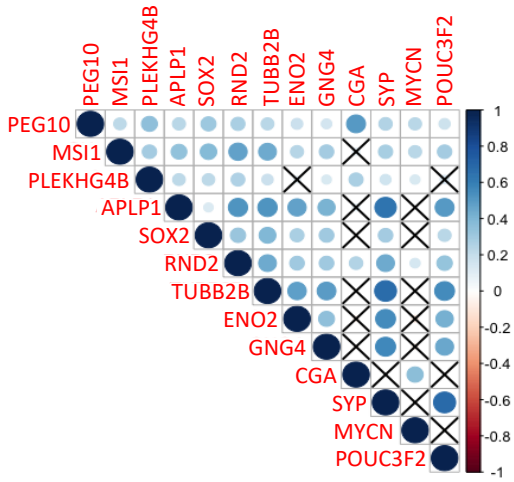

C

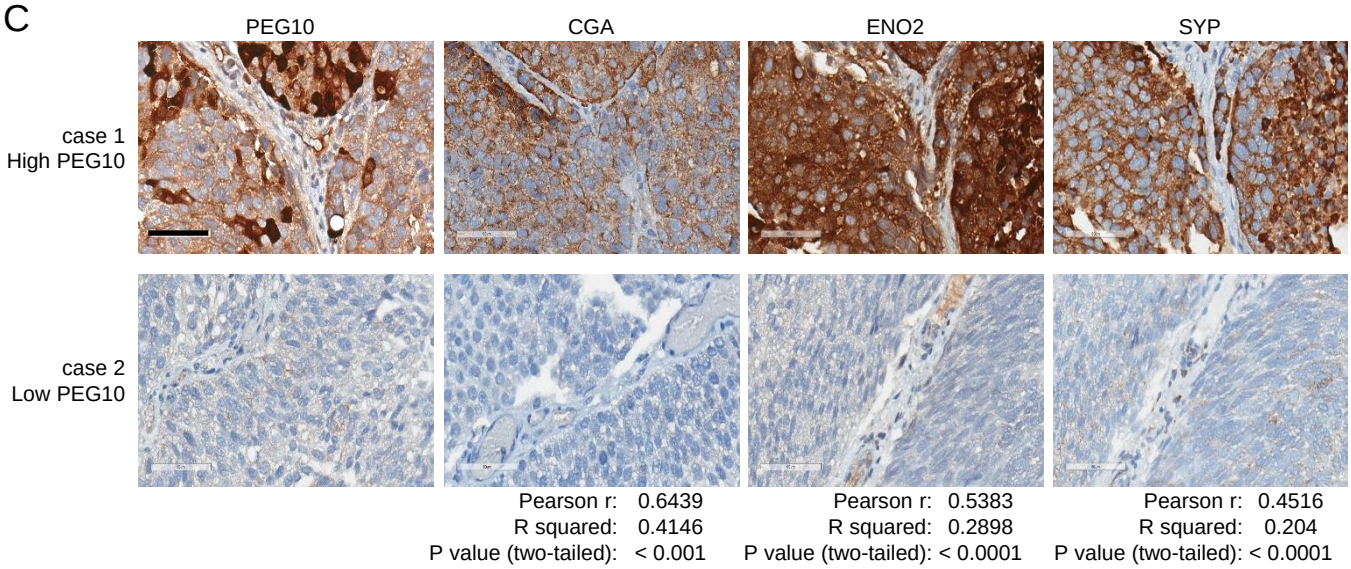

D

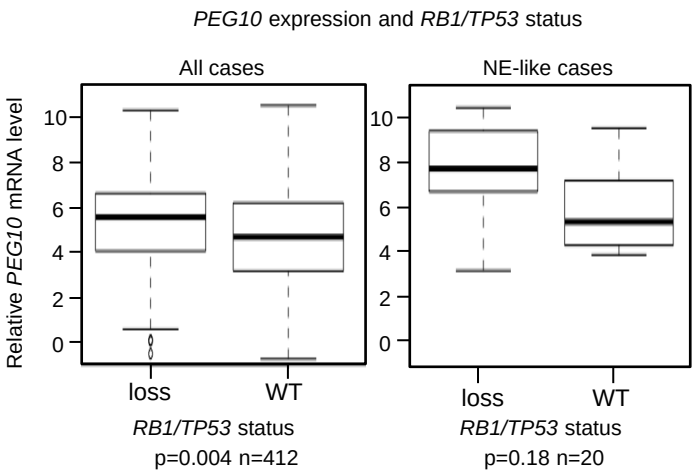

E

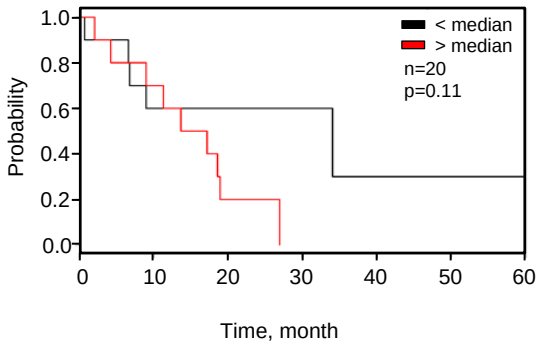

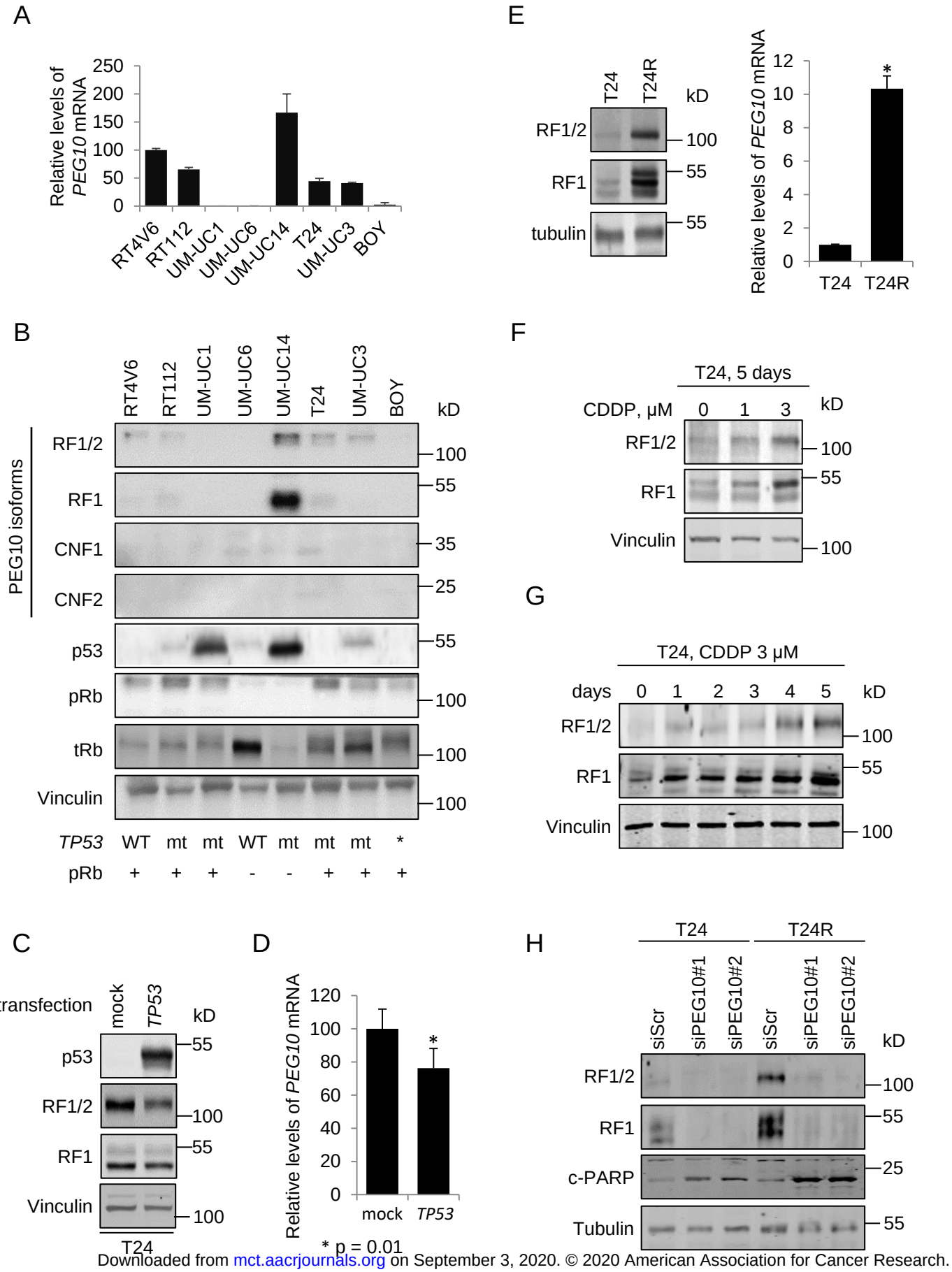

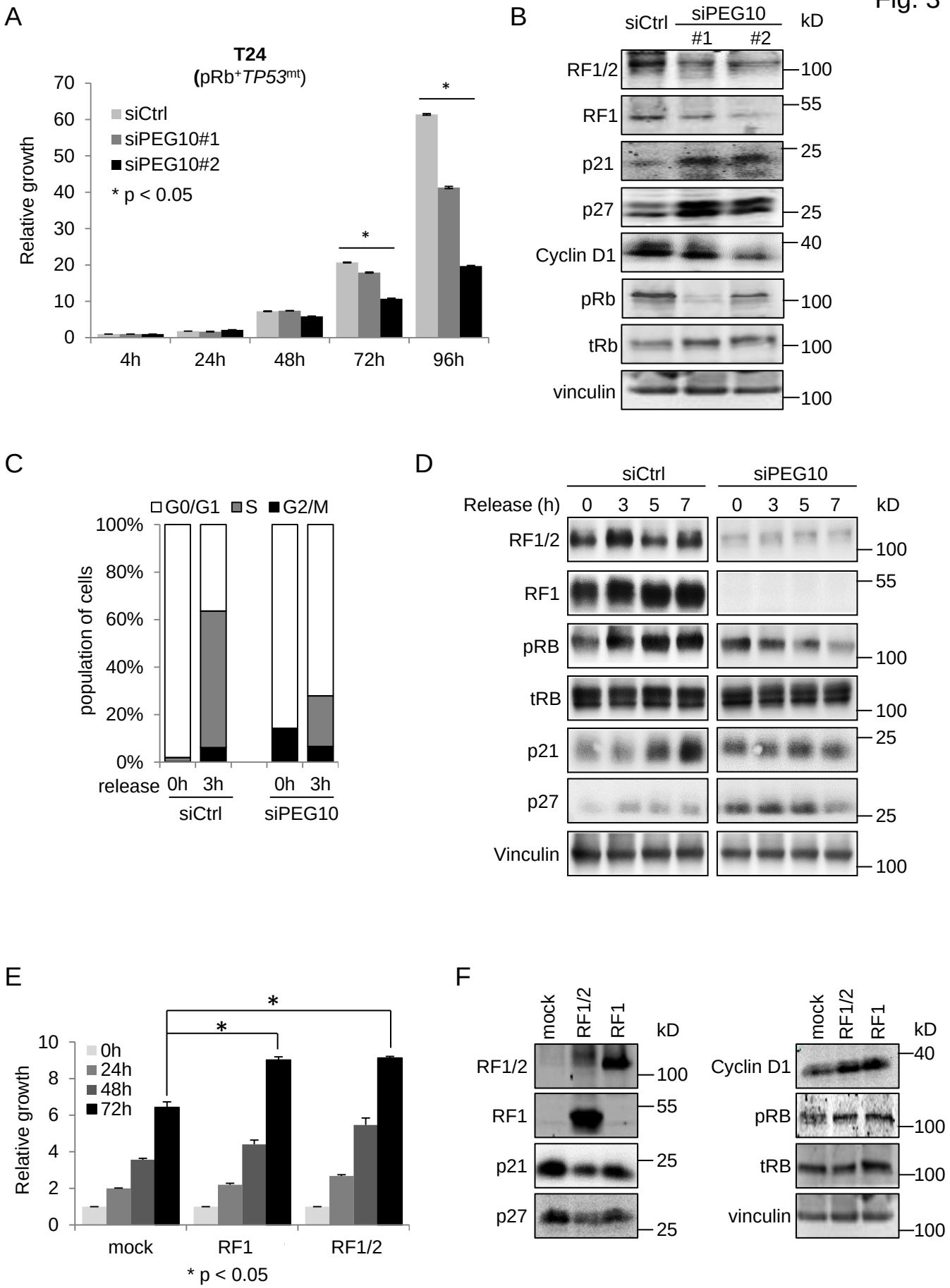

A

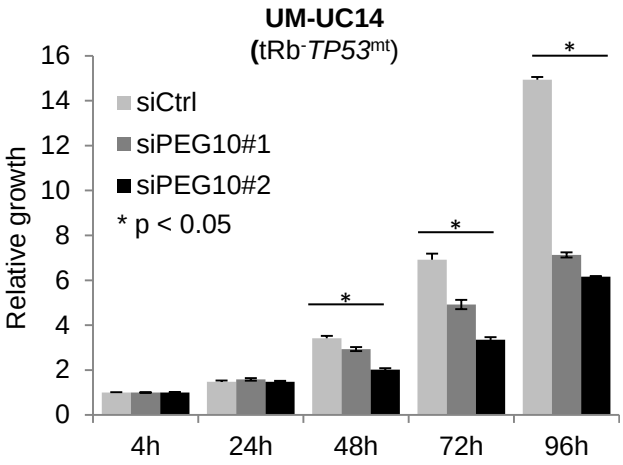

B

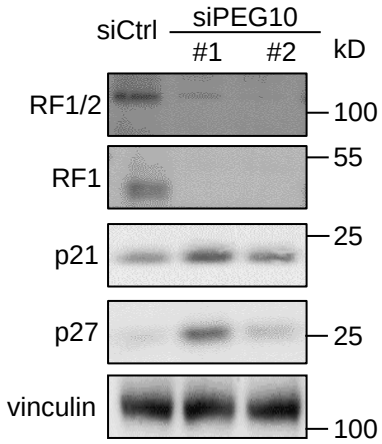

C

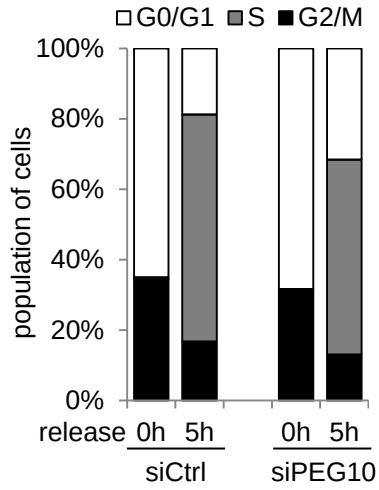

D

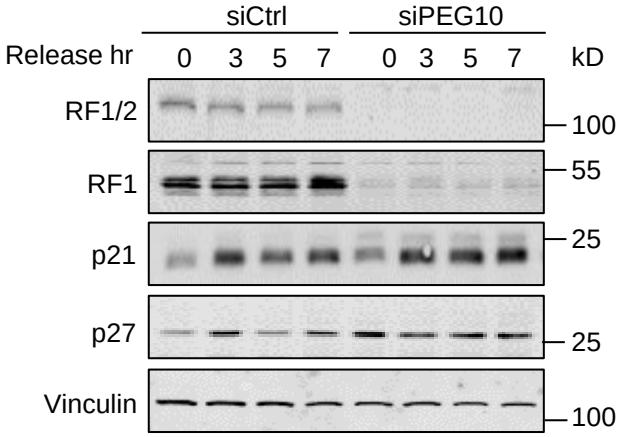

E

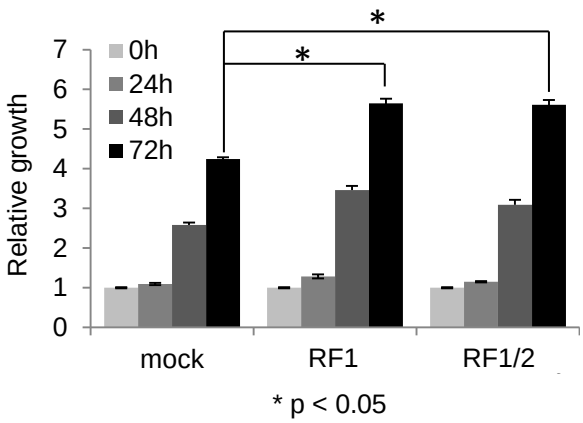

F

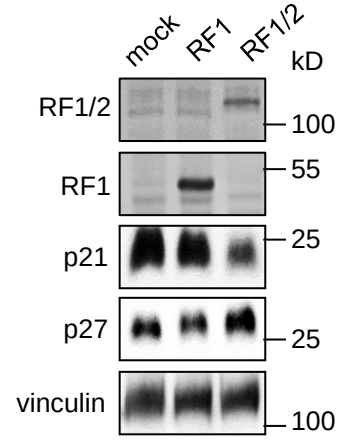

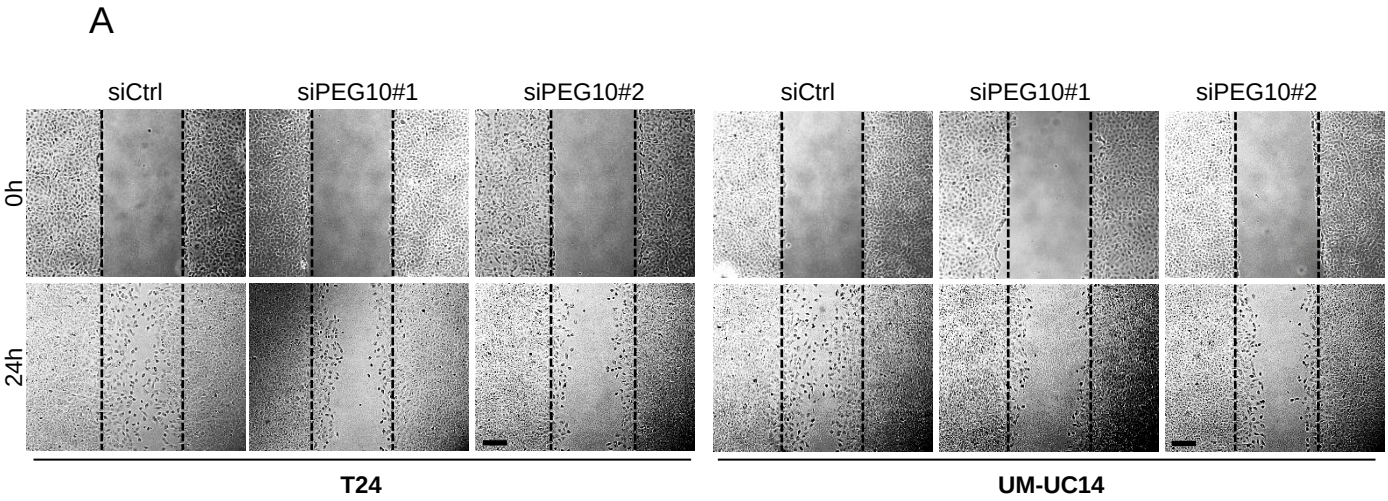

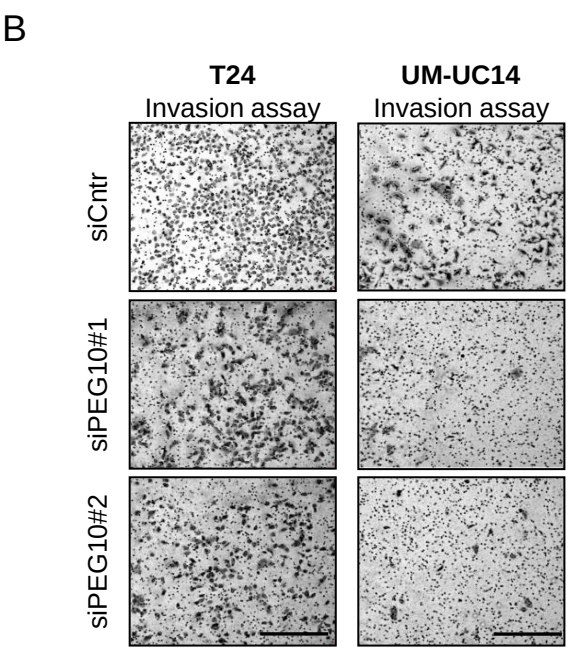

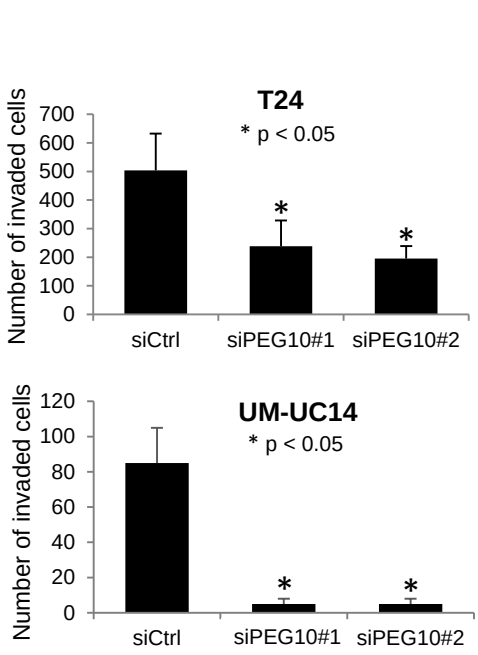

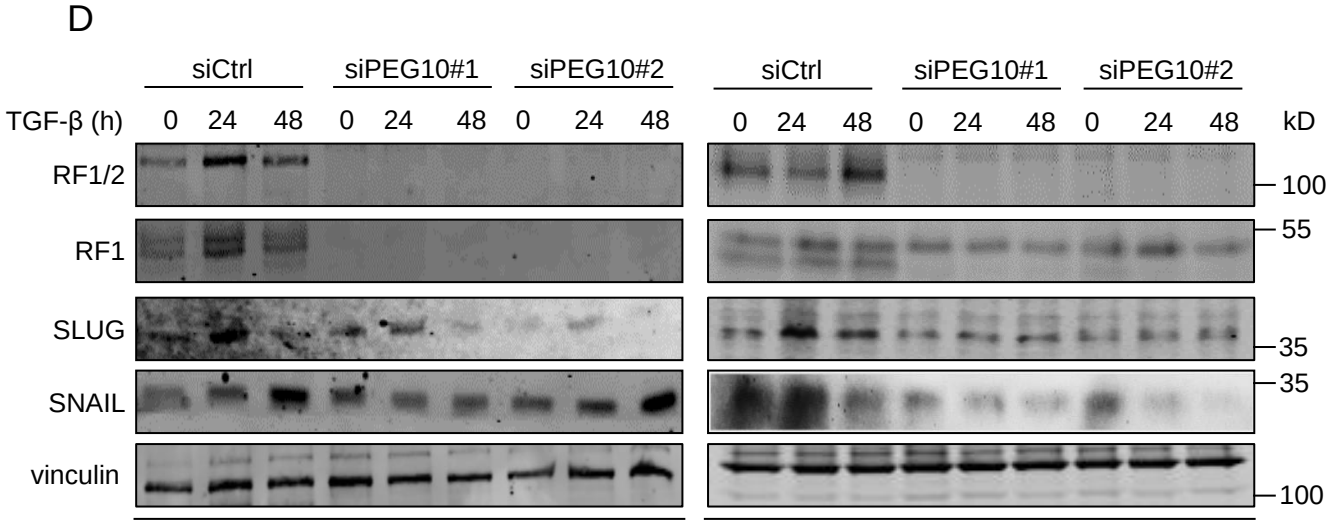

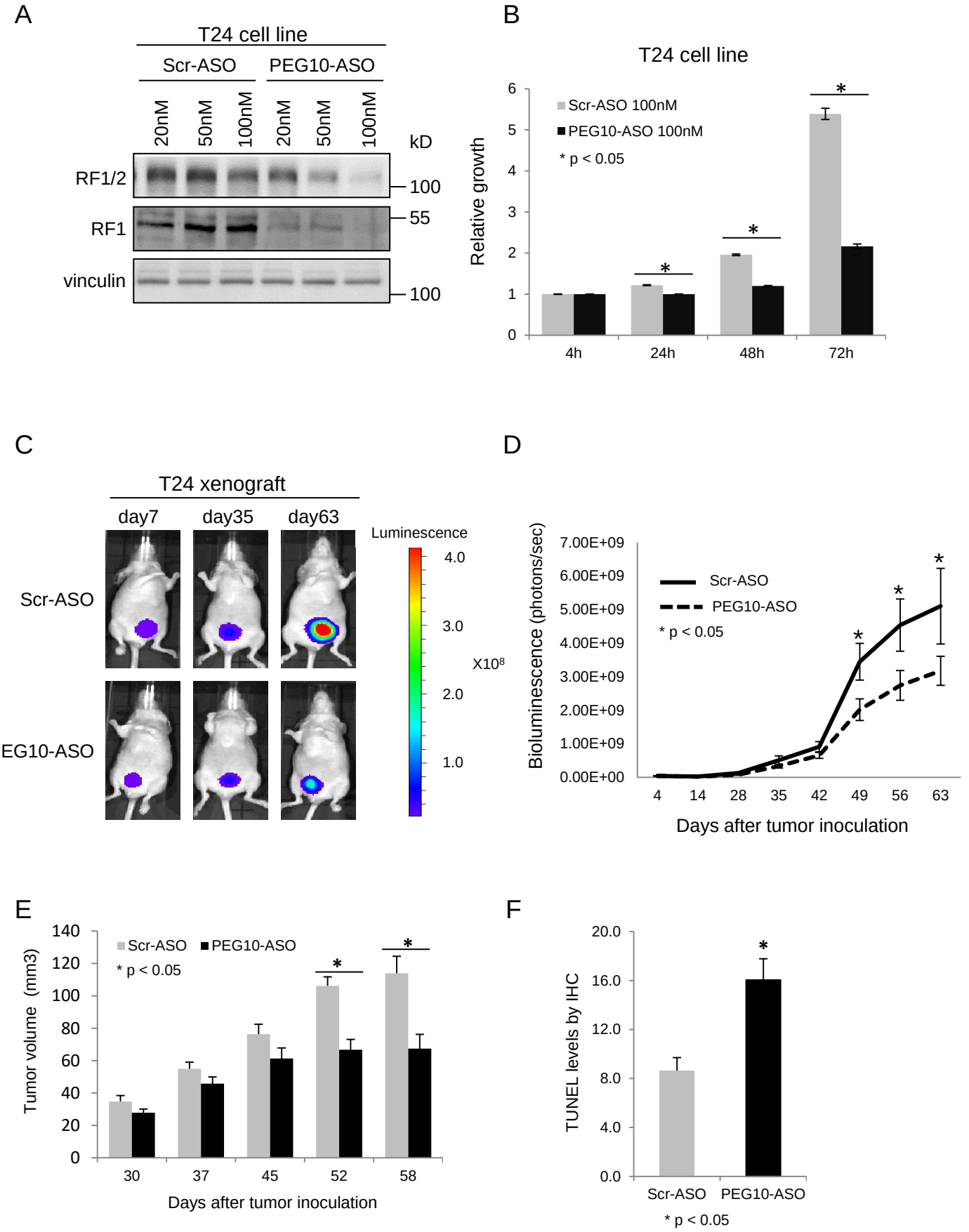

AACR American Association for Cancer Research

Molecular Cancer Therapeutics

Paternally Expressed Gene 10 (PEG10) Promotes Growth, Invasion and Survival of Bladder Cancer

Martin E. Gleave, Yoshihisa Kawai, Kenjiro Imada, et al.

Mol Cancer Ther Published OnlineFirst August 26, 2020.